Journal of Bioenergetics and Biomembranes, Vol. 19, No. 4, 1987

MINI-REVIEW

Electron Microscopy and Image Analysis of the Mitochondrial Outer Membrane Channel, VDAC

Carmen A. Mannella[1,2]

Received February 13, 1987

Abstract

The channel protein in the outer membrane of *Neurospora crassa* mitochondria, VDAC, forms extended planar crystals on the membrane. The arrays, which are induced by phospholipase A_2, are polymorphic, varying from parallelogram (P) to near-rectangular (R) geometry with increased phospholipase treatment. Computer-based analysis of projection images of negatively stained VDAC arrays indicates that the protein forms a transmembrane channel in the P array. Comparison of average images of arrays embedded in different negative stains suggests that the bore of the channel is 2–2.5 nm. The locations of functionally important lysine clusters on VDAC are inferred from the effects of succinylation on projection images of arrays negatively stained with phosphotungstate. Projection images of unstained frozen-hydrated arrays indicate the general shape of the channel and suggest each channel is formed by one 31-kDa VDAC polypeptide.

Key Words: Mitochondrial outer membrane; channel; electron microscopy; image processing; negative stain; frozen-hydrated; succinic anhydride.

Introduction

Electron microscopy has made several key contributions to the understanding of mitochondrial membrane structure. The best known example is the "head and stalk" subunit of negatively stained cristae, subsequently identified as F_1 ATPase (Fernandez-Moran, 1962; Parsons, 1963; Kagawa and

[1]Wadsworth Center for Laboratories and Research, New York State Department of Health, Empire State Plaza, Albany, New York 12201.
[2]School of Public Health Sciences, State University of New York at Albany, Albany, New York 12201.

0145-479X/87/0800-0329$05.00/0

Racker, 1966). Concurrent with the discovery of projecting inner membrane particles were observations of porelike subunits on the mitochondrial outer membrane (Parsons, 1963). In plant mitochondria, outer membranes have a pitted appearance in negative-stain electron micrographs (Parsons *et al.*, 1965). While the numerous stain-dense, 3-nm loci were attributed by some to an artifact of negative staining, those who first made the observations speculated that they might be channel openings in the membrane. The existence of pores in the mitochondrial outer membrane would explain this membrane's remarkable permeability to small molecules. However, identifying the negative stain subunits with a functional component of the mitochondrial outer membrane had to await advances in the assay of channel function.

With development of techniques for detecting pore formation in phospholipid membranes, it was found that mitochondria possessed a potent pore-former. This channel, first detected in protozoan mitochondria, was called VDAC, for voltage-dependent, anion-selective channel (Schein *et al.*, 1976). The channel exhibits multiple conductance states, switching from high (4.5 nS) to low (2.5 nS) conductance when transmembrane potentials exceed 20 mV. Furthermore, the channel displays higher permeabilities toward anions than cations. Colombini (1979) was the first to localize this channel-forming activity to the mitochondrial outer membrane in rat liver. Zalman *et al.* (1980) showed it to be associated with the major protein component of the outer membrane of plant mitochondria. X-ray scattering experiments had earlier implicated this trypsin-resistant, 30-kDa polypeptide as the main component of the subunits seen in negative-stain electron micrographs of this membrane (Mannella and Bonner, 1975).

The link between the functional entity, VDAC, and the subunits detected by electron microscopy was established with fungal mitochondria. In the mitochondrial outer membrane of *Neurospora crassa*, the 31-kDa VDAC polypeptide is the major protein component (Mannella, 1982; Freitag *et al.*, 1982). As with those of plants, outer membranes of *Neurospora* mitochondria show close-packed, stain-accumulating loci in negative-stain electron micrographs. However, unlike the plant subunits, those in fungal mitochondrial outer membranes tend to occur in periodic arrays (Mannella, 1982). Antibodies were raised against *Neurospora* mitochondrial outer membranes which were specific for the 31-kDa polypeptide and which inhibited incorporation of VDAC into planar bilayers (Mannella and Colombini, 1984). These antibodies bound to mitochondrial outer membranes and could be used to precipitate *Neurospora* mitochondria, unlike antibodies raised against SDS-solubilized VDAC (Freitag *et al.*, 1982). Indirect immunoelectron microscopy, using Protein A-colloidal gold as a marker, demonstrated that the anti-VDAC antibody bound specifically to mitochondrial outer membranes containing crystalline arrays of the stain-accumulating

subunits (Mannella and Colombini, 1984). This, together with observations that the 31-kDa VDAC polypeptide is the only polypeptide enriched in crystalline membrane fractions (Mannella, 1984), proved that the subunit arrays were composed of VDAC.

Formation of Periodic Channel Arrays

The tendency of VDAC to form crystalline arrays in the mitochondrial outer membrane of *Neurospora* is useful for electron microscopy, for reasons that will be explained below. It has been determined that channel arrays form on the mitochondrial outer membrane by the action of phospholipase A_2. Quantitative conversion of amorphous to crystalline outer membrane vesicles can be achieved by incubating dilute suspensions of the membranes with low levels of soluble phospholipase A_2 under continuous dialysis (Mannella, 1984). The subsequent decrease in surface area and increase in buoyant density of the membranes (Mannella, 1985) suggests that ordered packing of channels is associated with release of the products of phospholipid hydrolysis from the membrane. The frequent occurrence of subunit-free membrane regions contiguous with ordered channel arrays in these membrane fractions suggests that the crystallization process also involves lateral phase separation of membrane components (Mannella, 1982).

Mitochondrial outer membranes have an endogenous phospholipase A activated by micromolar Ca^{2+} (Douce *et al.*, 1968; Vignais *et al.*, 1969), suggesting that organization of the channels into close-packed arrays might occur *in vivo*, perhaps as a response to elevated Ca^{2+}. *In vitro* experiments indicate that endogenous phospholipase is capable of inducing formation of channel arrays on the outer membranes of intact mitochondria. For example, preincubation of *Neurospora* mitochondria with 5–50 μM $CaCl_2$ prior to outer membrane isolation greatly increases the number of channel arrays subsequently observed in the absence of added phospholipase A_2 (Mannella, unpublished observation). The functional consequence of the ordered aggregation of mitochondrial outer membrane channels are unknown at this time. It has been demonstrated with acetylcholine receptors that clustering of channels can significantly alter their kinetic charcteristics (Young and Poo, 1983).

Structural Information from Electron Microscopic Image Analysis

Image processing techniques have been applied to transmission electron micrographs of outer mitochondrial membrane arrays to derive basic

structural parameters of crystalline VDAC. Substructure in an image of a negatively stained, flattened, array-bearing vesicle (Fig. 1A) is difficult to interpret directly. Information from the two membrane layers is superimposed in projection images, along with background contributions from the carbon support film. Fourier filtration (DeRosier and Klug, 1968) is used to compute noise-free averages of each crystalline layer in these membranes. The image is digitized (with a scanning microdensitometer) and its Fourier transform computed. The power spectrum of the transform is equivalent to the optical diffraction pattern of Fig. 1C. The transform consists of discrete reflections on two different parallelogram lattices, corresponding to the two periodic membrane layers, plus amorphous scattering arising from random image components (noise). The spatial separation of ordered and random image components in Fourier space is the basis of the filtration. The transform is masked so that Fourier components corresponding to only one membrane lattice are passed, and the inverse transform is calculated. The result is a "filtered" image, an average of the projected density in one negatively stained membrane layer, free of random noise and of contributions from the other layer (provided reflections on the two lattices do not anywhere overlap).

Fourier averages of negatively stained parallelogram VDAC arrays are shown in Figs. 1B and 2A. The repeat unit contains six sites of negative stain accumulation with 4.5–5 nm center-to-center separation of nearest neighbors. The stain centers are arranged on a hexagon with two-fold rotational symmetry and these repeat units are in turn aligned on a parallelogram lattice of dimensions 13.3 × 11.5 nm, with a lattice angle of 109°

The arrays of VDAC observed in mitochondrial outer membrane fractions are polymorphic, the most common being the parallelogram (P) array just described. With increased phospholipase A_2 treatment, another array predominates, a near-rectangular (R) array with a smaller unit cell (8.4 × 5.1 nm) which contains only two stain centers (Mannella *et al.*, 1983; Mannella, 1984, 1985). The lateral rearrangement of subunits involved in the transition from P to R geometry is diagramed in Fig. 2. The coordination between the subunits in the P and R lattices differs significantly, raising the possibility that the VDAC protein may be in different conformations in the two arrays (see below).

Channel Shape and Size

The diameters of the stain centers in filtered images of VDAC arrays fall in the range estimated for the bore of the VDAC channel based on different functional characteristics, 2–4 nm (Colombini, 1985; Benz, 1985).

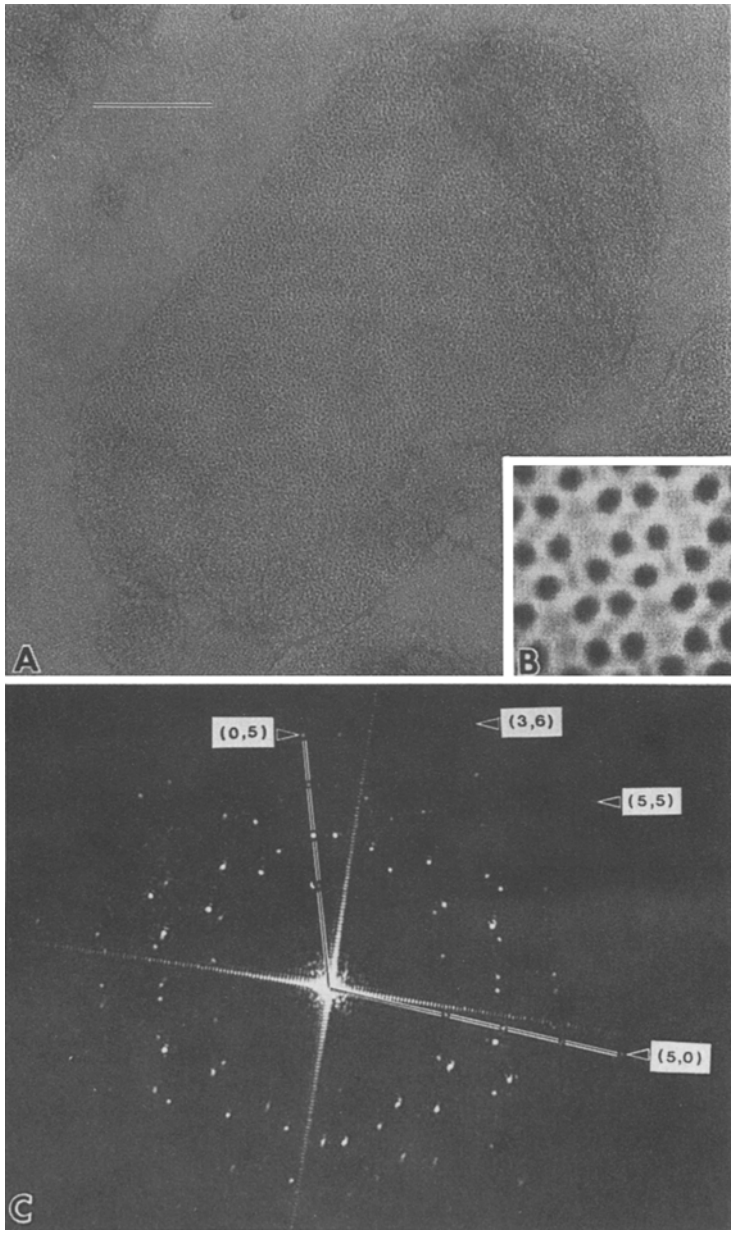

Fig. 1. (A) Electron micrograph of a fungal mitochondrial outer membrane containing a periodic VDAC array, negatively stained with uranyl acetate. Scale bar = 100 nm. (B) Fourier average of a 23 × 23 nm^2 area of one of the two superimposed arrays in the image of (A). (C) Optical diffraction (obtained with coherent illumination from a He–Ne laser) from a 170-nm square region at the center of the micrograph in (A). The principal axes ($h,0$ and $0,k$) of the lattice used for the filtration in (B) are indicated, as are several high-resolution reflections. Reproduced from Mannella (1982) by permission of The Rockefeller University Press.

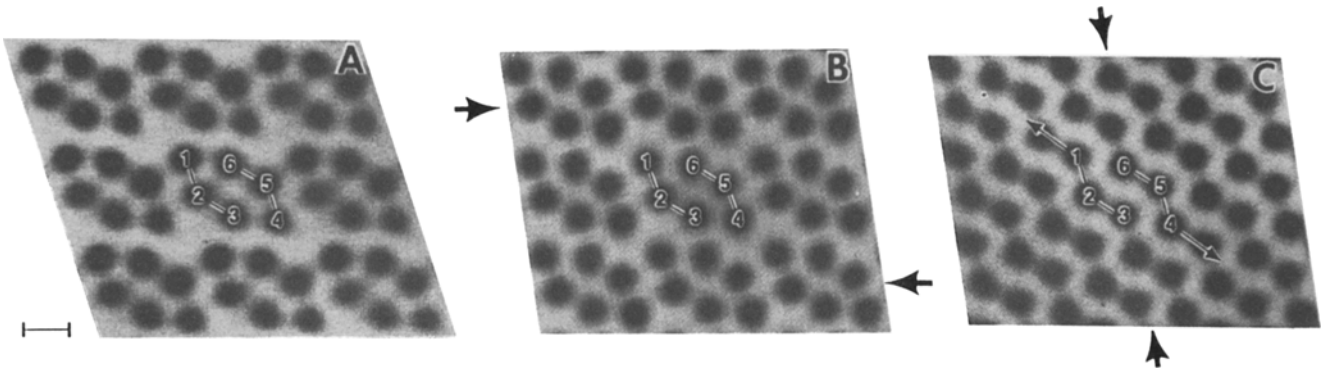

Fig. 2. Fourier-filtered images of phosphotungstate-stained VDAC arrays showing the transition from parallelogram (P) to near-rectangular (R) geometry associated with increasing phospholipase A_2 treatment. (A) Region of P array containing nine unit cells. The six stain-filled channels in the central repeat unit are numbered for reference. (B) An array with geometry intermediate between P and R arrays. Adjacent horizontal rows have slid 1 nm in the directions indicated by the arrows, resulting in a decrease in the lattice angle from 109 to 99°. (C) Equivalent region of R array. The lattice has decreased by 0.7 nm in the direction of the large arrows, compared with the P lattice in A. Also the hexagonal group of channels in the repeat unit has split into two triplets, offset 0.8 nm in the direction indicated by the small arrows relative to their positions in (A) and (B). Scale bar in (A) = 5 nm. Reproduced from Mannella *et al.* (1983).

This observation provokes the question of whether these dense strain centers represent projections of transmembrane channels. Information about the distribution of stain in the vertical direction of the arrays is needed to answer this question. Three-dimensional reconstruction from electron microscopic projections of tilted specimens is possible using either Fourier- or direct-space (modified back-projection) algorithms (Amos *et al.*, 1982; Gilbert, 1972). Application of both techniques to tilt-series projection data from P arrays indicates that the stain at each of the six loci in the unit cell spans the 5–6-nm-thick membrane (Mannella *et al.*, 1984). Recently completed Fourier analysis of the three-dimensional density distribution in the R array shows the stain penetrating only about halfway into the membrane (Mannella and Frank, unpublished). Thus the P and R arrays of the VDAC protein may correspond to the open and closed states of the channel.

Inferring the bore of the channel from averaged projections of negatively stained VDAC arrays is complicated by the stain dependence of the projected channel diameters: 3–3.5 nm with phosphotungstate, 2–2.5 nm with uranyl salts. This discrepancy has been attributed to the tendency of commonly used negative stains to positively stain proteins (Mannella and Frank, 1984). Penetration of stain into the protein wall of a channel will make the channel look wider in projection than it actually is. The negative stain aurothioglucose was used to resolve this issue. Unlike heavy-metal salts, this gold-tagged sugar is totally uncharged and not expected to positively stain any membrane component. The average diameter of projections of mitochondrial outer membrane channels embedded in aurothioglucose is close to 2 nm (Mannella *et al.*, 1986), favoring the lower estimate of channel size.

Chemical Modifiers and Effectors

Reaction of VDAC with succinic anhydride has been shown to dramatically alter the functional characteristics of the channel. Voltage dependence is lost and ion selectivity switches from anionic to cationic, although channel conductance is unchanged (Doring and Colombini, 1985). These effects have been interpreted to indicate the involvement of lysines in both the voltage-sensing and ion-selectivity mechanisms of the channel protein (Colombini, 1985). The VDAC polypeptide contains numerous lysine residues (26 in *Neurospora*; Freitag *et al.*, 1982) which normally carry a $+1$ charge and which is changed to -1 by succinylation. To determine the effects of succinylation on the structure of VDAC, crystalline arrays of the channel were reacted with succinic anhydride prior to negative staining with phosphotungstate and uranyl acetate (Mannella and Frank, 1984). Chemical modification does not detectably alter the lattice parameters of arrays

embedded in either stain, suggesting that functional changes elicited by succinylation are not associated with large-scale changes in channel conformation. However, the lateral distribution of one of the stains on the VDAC arrays was significantly altered by pretreatment with succinic anhydride. The stain affected was phosphotungstate, a complex anion known to positively stain basic amino acids in proteins (Tzaphlidou *et al.*, 1982). Analysis of differences between average projections of control and succinylated VDAC arrays (Mannella and Frank, 1984, 1987a) provides a tentative localization of the sites of exposed clusters of basic amino acids on the VDAC molecule.

A synthetic polyanion has been shown to reduce the permeability of VDAC in bilayers (Yeung *et al.*, 1986). This copolymer of styrene, maleate, and methacrylate (3 : 2 : 1) has been found to cause rapid loss of long-range order in VDAC crystals, as do other polyanions, such as polyglutamate and poly(glutamate, alanine) (Mannella and Frank, 1987b). The disordering effect of polyanions on the VDAC arrays is consistent with a conformational change in the channel, e.g., from an open to partially closed state as suggested by the change in channel conductance. Alternatively, loss of crystalline order may be caused by disruption by the polyanions of interactions between the components of the arrays. Phospholipases C and D, which hydrolyze the polar head groups from phospholipids, also disorder the VDAC arrays (Mannella, 1986). This result suggests that electrostatic interactions between zwitterionic phospholipids and the VDAC polypeptide are critical for maintenance of long-range order in the arrays.

Structure of Frozen-Hydrated Crystalline VDAC

Negative stains are used in electron microscopy because they confer increased contrast and resistance to radiation damage on biological specimens. However, the use of negative stains has its drawbacks. Attainable resolution in electron images of negatively stained objects is limited to about 2 nm. Also, the structural information provided is primarily topological, mixed to varying degrees with positive staining effects (see above). Advances in imaging of unstained macromolecule complexes have been made in the past decade which overcome these shortcomings. Electron images and diffraction patterns containing high-resolution information can be recorded from specimens embedded in low-density media provided care is taken to minimize the radiation dose to the specimens (Unwin and Henderson, 1975). Techniques are becoming almost routine for the preparation and imaging of unstained specimens embedded in vitreous ice by rapid freezing at liquid-nitrogen temperature (Taylor and Glaeser, 1976; Adrian *et al.*, 1984). Such

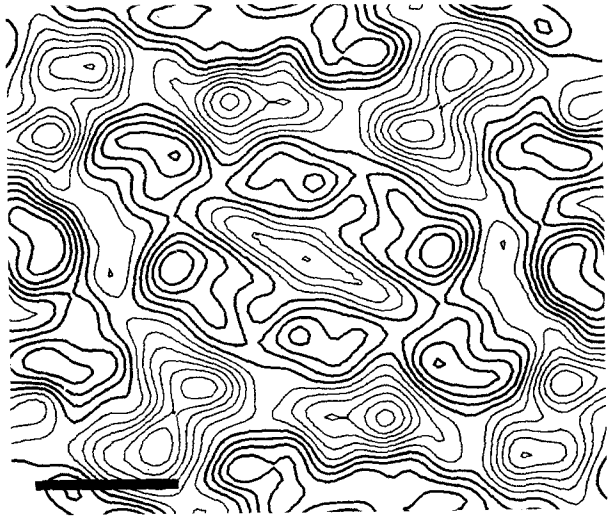

Fig. 3. Projected density of unstained, frozen-hydrated crystalline VDAC, obtained by correlation averaging (Mannella *et al.*, 1986). Dark contours represent high density (protein) and light contours low density (lipid). Two-fold rotational symmetry imposed. Scale bar = 5 nm.

frozen-hydrated specimens are in an essentially native environment and are about five times less susceptible to deleterious effects of the electron beam than equivalent specimens at room temperature (Glaeser and Taylor, 1978; LePault *et al.*, 1983). Because of the absence of stain, components within membranes can be directly visualized, with contrast provided by the inherent density differences between protein and lipid.

Figure 3 is an average of unstained crystalline VDAC obtained from frozen-hydrated *Neurospora* mitochondrial outer membranes (Mannella *et al.*, 1986). Image analysis in this case involved correlation averaging, a procedure which corrects for lattice disorder in imperfect planar crystals (Saxton, 1980; Frank, 1982). A Fourier average of a locally well-ordered part of an array was cross-correlated with the entire membrane. Peaks occur in the resulting cross-correlation function wherever there is a close match between the field and the Fourier-filtered reference. The projected density map of Fig. 3 was obtained by summation of small areas windowed from the field at these peak positions. The six channel positions in the unit cell are occupied by protein (high density) subunits surrounded by lipid (low-density). Each subunit is shaped like a "C", with an arm extending from a dense locus. Comparison of this unstained average with negative-stain averages indicates that the pore is located in the less-dense region inside each "C." The channel interior is not better defined because of the low effective resolution of this average, between 2.5 and 3 nm.

Experiments are in progress to improve the resolution in averaged projections of frozen-hydrated crystalline VDAC, to be followed by three-dimensional reconstruction of the channels in both the P and R arrays. Since the two polymorphs appear to represent open and closed states of the channel, comparison of the three-dimensional structure of the VDAC protein in both types of arrays may provide insight into the mechanism of closure of this channel.

Number of VDAC Polypeptides per Channel

In addition to indicating the shape of the protein subunits of VDAC, the moderate-resolution projected density map of Fig. 3 can be used to estimate the relative surface area occupied by protein and lipid in the P array. In Fig. 3, protein and lipid are demarcated at the density level in the contour map at which the protein subunits within the unit cell begin to touch. For this choice of protein outline, 48% of the surface area of the array is occupied by lipid. The volume occupied by protein within one unit cell of the P array can then be estimated from the known lattice parameters assuming (1) the channel height is equal to that of the bilayer, 5 nm, based on structural evidence and the insensitivity of the protein to protease (Mannella, 1981; Mannella *et al.*, 1986; Freitag *et al.*, 1982); (2) channel shape is uniform in the transverse direction; and (3) the interior aqueous compartment of each channel in the P array is a right circular cylinder of diameter 2.0–2.5 nm (Mannella *et al.*, 1984, 1986). Under these assumptions, the total volume occupied by protein in the unit cell of the P array is $255 \pm 26\,nm^3$. The partial specific volume of the 31-kDa fungal VDAC polypeptide can be estimated from its amino acid composition (Freitag *et al.*, 1982) to be $0.736\,cm^3/g$ (Cohn and Edsall, 1943). It is then a simple matter to calculate that, within the framework of the above estimates, there are 6.7 ± 0.7 VDAC polypeptides per unit cell in the P array—or very nearly 1 polypeptide per channel opening.

Model studies indicate that a single yeast VDAC polypeptide is sufficient to form a channel with dimensions like those expected for VDAC (Forte *et al.*, 1987). Results of hydrodynamic experiments indicate that detergent extracts of rat-liver VDAC contain primarily dimers of the 31-kDa polypeptide (Linden and Gellerfors, 1983). Since such extracts show exclusively single-channel insertions in bilayers, this suggests that the functional unit of rat-liver VDAC is a dimer. These results raise the possibility that, despite functional similarities, there may be fundamental structural differences between VDAC of fungi and mammals (see Mannella *et al.*, 1984).

Acknowledgments

The contributions of the following to the research summarized in this report are gratefully acknowledged: Drs. J. Frank, M. Radermacher, and M. Colombini; also B. Cognon, A. Ribeiro, and D. D'Arcangelis. This material is based upon work supported by grants PCM-8021789, PCM-8313045, and PCM-8315666 from the National Science Foundation.

References

Adrian, M., Dubochet, J., Lepault, J., and McDowall, A. W. (1984). *Nature (London)* **308**, 32–36.

Amos, L. A., Henderson, R., and Unwin, P. N. T. (1982). *Prog. Biophys. Mol. Biol.* **39**, 183–231.

Benz, R. (1985). *CRC Crit. Rev. Biochem.* **19**, 145–190.

Cohn, E. J., and Edsall, J. T. (1943). In *Proteins, Amino Acids and Peptides as Ions and Dipolar Ions* (Cohn, E. J., and Edsall, J. T., eds.), Reinhold, New York, pp. 370–381.

Colombini, M. (1979). *Nature (London)* **279**, 643–645.

Colombini, M. (1985). In *Ion Channel Reconstitution* (Miller, C., ed.), Plenum Press, New York and London, pp. 533–552.

DeRosier, D. J., and Klug, A. (1968). *Nature (London)* **217**, 130–134.

Doring, C., and Colombini, M. (1985). *J. Membr. Biol.* **83**, 81–86.

Douce, R., Guillot-Salomon, T., and Lance, C. (1968). *Bull. Soc. Fr. Physiol. Veg.* **14**, 351–373.

Fernandez-Moran, H. (1962). *Circulation* **26**, 1039–1065.

Forte, M., Guy, H. R., and Mannella, C. A. (1987). *J. Bioenerg. Biomembr.* **19**, 341–350.

Frank, J. (1982). *Optik* **63**, 67–89.

Freitag, H., Neupert, W., and Benz, R. (1982). *Eur. J. Biochem.* **123**, 629–639.

Gilbert, O. C. F. (1972). *Proc. R. Soc. London B* **182**, 89–102.

Glaeser, R., and Taylor, K. (1978). *J. Microsc.* **112**, 127–138.

Kagawa, Y., and Racker, E. (1966). *J. Biol. Chem.* **241**, 2475–2482.

Lepault, J., Booy, F. P., and Dubochet, J. (1983). *J. Microsc.* **129**, 89–102.

Linden, M., and Gellerfors, P. (1983). *Biochim. Biophys. Acta* **736**, 125–129.

Mannella, C. A. (1981). *Biochim. Biophys. Acta* **645**, 33–40.

Mannella, C. A. (1982). *J. Cell Biol.* **94**, 680–687.

Mannella, C. A. (1984). *Science* **224**, 165–166.

Mannella, C. A. (1985). *Methods Enzymol.* **125**, 595–610.

Mannella, C. A. (1986) *Biochim. Biophys. Acta* **861**, 67–73.

Mannella, C. A., and Bonner, W. D., Jr. (1975). *Biochim. Biophys. Acta* **413**, 226–233.

Mannella, C. A., and Colombini, M. (1984). *Biochim. Biophys. Acta* **774**, 206–214.

Mannella, C. A., and Frank, J. (1984). *Ultramicroscopy* **13**, 93–102.

Mannella, C. A., and Frank, J. (1987a) *J. Ultrastruct. Molec. Struct. Res.*, in press.

Mannella, C. A., and Frank, J. (1987b). *Biophys. J.* **51**, 230a.

Mannella, C. A., Colombini, M., and Frank, J. (1983). *Proc. Natl. Acad. Sci. USA* **80**, 2243–2247.

Mannella, C. A., Radermacher, M., and Frank, J. (1984). In *Proceedings of the Electron Microscope Society of America* (Bailey, G. W., ed.), San Francisco Press, San Francisco, pp. 644–645.

Mannella, C. A., Ribeiro, A., and Frank, J. (1986). *Biophys. J.* **49**, 307–318.

Parsons, D. P. (1963). *Science* **140**, 985–987.

Parsons, D. P., Bonner, W. D., Jr., and Verboon, J. G. (1965). *Can. J. Bot.* **43**, 647–655.

Saxton, W. O. (1980). In *Electron Microscopy at Molecular Dimensions* (Baumeister, W., and Vogell, W., eds.), Springer-Verlag, Berlin, pp. 244–255.
Schein, S. J., Colombini, M., and Finkelstein, A. (1976). *J. Membr. Biol.* **30**, 99–120.
Taylor, K., and Glaeser, R. M. (1976). *J. Ultrastruct. Res.* **55**, 448–456.
Tzaphlidou, M., Chapman, J. A., and Meek, K. M. (1982). *Micron* **13**, 119–131.
Unwin, P. N. T., and Henderson, R. (1975). *J. Mol. Biol.* **94**, 425–440.
Vignais, P. M., Nachbauer, J., and Vignais, P. V. (1969). In *Mitochondria: Structure and Function* (Ernster, L., and Drahota, Z., eds.), Academic Press, London and New York, pp. 43–58.
Yeung, C. L., Tung, J., Colombini, M., and Konig, T. (1986). *Biophys. J.* **49**, 206a.
Young, S. H., and Poo, M. (1983). *Nature (London)* **304**, 161–163.
Zalman, L. S., Nikaido, H., and Kagawa, Y. (1980). *J. Biol. Chem.* **255**, 1771–1774.